ARTICLE TEMPLATE

State Observation of Unknown Nonlinear SISO Systems based on Virtual Input Estimation

Fawzia Amokrane[a], Emmanuel Piat[a], Joël Abadie[a], Adrien Drouot[a] and Juan Escareno[b]

[a]FEMTO-ST institute, Univ. Bourgogne Franche-Comté, CNRS, 15B avenue des Montboucons, 25030 Besançon, cedex, France
[b]Univ. Limoges, CNRS XLIM, UMR 7252, F-87000 Limoges, France

ARTICLE HISTORY
Compiled February 5, 2020

ABSTRACT
This paper introduces a generic procedure for the state estimation of unknown nonlinear SISO systems, i.e. when no information is available on their structure, possibly time-varying parameters and potential disturbances. This procedure relies on the choice of an arbitrary linear model and the use of a Generic Linear Extended State Observer, whose principle is also introduced in the paper. The proposed approach overcomes well-known model-based nonlinear techniques in the sense that it is easy to implement, all the while avoiding any identification step and mathematical complexity. Simulation results involving a nonlinear system, subject to external disturbances and measurement noise, compare the performance of the proposed approach to the one of some model-free nonlinear observers described in the literature.

KEYWORDS
Observer for Unknown Nonlinear Systems, Extended State Observer, ADRC.

1. Introduction

Owing to its importance in modern control theory, the field of state observation for dynamical systems has been an active area of research for decades. Based only on the inputs and outputs of any given system, the resulting observers are expected to produce an estimation of the states, that is then used by the control structure. For linear systems, one can cite the works of Kalman for stochastic systems (Kalman, 1960) and Luenberger for deterministic systems (Luenberger, 1964). However, physical systems may feature some unexpected complexity due to, e.g., inherent nonlinearities, unavoidable and unknown changes of their structure (uncertainties), the influence of the environment (disturbances), etc. Therefore, these systems are no longer linear and that is why many theoretical and practical developments focus on the design of nonlinear observers.

There exist various strategies for the design of observers for nonlinear systems. There are, for example, the extended Kalman filter or one of its many extensions (Julier and Uhlmann, 1997), Lie algebra-based observers (Gauthier, Hammouri,

CONTACT Fawzia Amokrane. Email: fawzia.amokrane@femto-st.fr

& Othman, 1992; Krener and Isidori, 1983), Luenberger-like observers (Marconi, Praly, & Isidori, 2007; Zeitz, 1987), optimisation-based observers (Dong, Wang, & Wang, 2013), high-gain observers (Khalil and Praly, 2013), etc. Of all of the above approaches, the high-gain observers have received the most attention due to their simplicity and good performance in noise-free settings (Khalil and Praly, 2013). Indeed, in the high-gain observers paradigm, the estimation error trajectory has an exponential decay rate that can be chosen arbitrarily fast by acting on a design parameter that appears in the observers structure. Nevertheless, the high-gain observers design also highlights drawbacks, including implementation issues due to the value of the design parameter, the peaking phenomenon during the transient and a sensitivity to measurement noise (Astolfi, 2016). Recent works alleviated these undesirable properties (Astolfi, Marconi, Praly, & Teel, 2018), but this has been achieved at the cost of a more complicated design, i.e. increase of the observers dimension to $2n-1$, use of saturation functions in the observers dynamics, etc.

Furthermore, a major limitation that is common to all the above approaches is that they all require some a priori information on the structure of the systems, e.g. their order, a Lipschitzian behaviour (Astolfi et al., 2018; Khalil and Praly, 2013), a stable zero dynamics (Freidovich and Khalil, 2008), etc. However in many industrial cases, the systems cannot be a priori known, neither theoretically nor experimentally, but still require efficient observation and control schemes. Also, as the mathematical complexity inherent to the nonlinear nature of the systems may be an issue, there is a growing interest in the development of accessible and general methods to solve the problem of state observation and control of such unknown nonlinear systems. Owing to its less dependence on systems information, its abilities to cope with a wide range of uncertainties and disturbances, and its simplicity in the control structure, the Active Disturbance Rejection Control (ADRC) framework (Gao, Huang, & Han, 2001; Gao, 2006; Guo and Zhao, 2016) is a significant step towards this purpose. This framework clearly inspired the approach proposed in this paper.

The idea of ADRC consists in estimating both the state and a total disturbance, that lumps unmodeled dynamics and external disturbances into an extended state, by an Extended State Observer (ESO) (Han, 1995). Thus, the state of the unknown systems becomes available for control purposes and the total disturbance can be compensated for in real time. Following the ESO parameterisation steps described in (Gao, 2003), the ADRC technique has been used to solve various kinds of engineering problems, e.g., motor control (Feng, Liu, & Huang, 2004), flight control (Xia, Zhu, Fu, & Wang, 2011), robot control (Talole, Kolhe, & Phadke, 2010), etc. Yet, many of the ESO developed in the literature like the Standard Linear Extended State Observer (SLESO) (Kim, Rew, & Kim, 2010; Li, Yang, Chen, & Chen, 2012, 2014; Talole et al., 2010; Wang, Li, Yang, Wu, & Li, 2015) are of order $n+1$, where n is the order of the system. This implicitly assumes that the total disturbance is constant or slowly time-varying. Therefore, in the common case of non constant total disturbance, the quality of the estimation provided by the standard ESO becomes insufficient (Madoński and Herman, 2015). In order to improve the efficiency of the ESO, a possible option is to increase their order and that idea paved the way to the design of higher-order ESO (Godbole, Kolhe, & Talole, 2013; Madoński and Herman, 2013, 2015) and Generalised Proportional Integral observers (GPI) (Luviano-Juárez, Cortés-Romero, & Írez, 2010; Sira-Ramírez, Luviano-Juárez, Ramírez-Neria, & Zurita-Bustamante, 2017). Indeed, increasing the number of extended states allows

to effectively reconstruct a total disturbance described by complex and sophisticated high order polynomial.

This paper addresses the on-line state observation problem of a specific class of nonlinear SISO systems that are totally unknown. No learning method is used in contrast to identification and control approaches based on artificial neural networks (Suykens, Vandewalle, & De Moor, 1996). In the proposed procedure, the unknown nonlinear system is represented as a chosen (arbitrarily because no information is provided) linear system to which is added an unknown non physical exogenous input, called a *virtual input*. That exogenous input can be seen as an alternative to the total disturbance of the ADRC framework. Indeed, the virtual input gathers all the neglected nonlinearities, unmodeled dynamics, parameter uncertainties, and external disturbances such that the input-output dynamics of the linear system matches the one of the nonlinear system. Then, extending the state of the linear system with some well-posed linear combinations involving that unknown virtual input, its time evolution can be estimated with any linear extended state observation technique, alongside with the state of the system. In this paper, this will be achieved by a Generic Linear Extended State Observer (GeLESO). This new concept is a less conservative version of higher-order ESO and GPI observers used in ADRC in the sense that the GeLESO is built upon a linear system whose parameters are not necessarily restricted to zero as it is the case for higher-order ESO and GPI observers. Furthermore, the order of this observer can be increased at will in order to preserve the estimation accuracy even with unknown complex virtual input. In the following, the design procedure of the GeLESO is described. The proof of the interest of increasing its order is established. Its performance is validated by simulations and its behaviour is compared to higher-order ESO/GPI observers when measurement noises are present or not.

The remainder of the paper is organised as follows. Section 2 defines the framework of the approach and specifies the class of nonlinear systems that are considered. Section 3 proves that these nonlinear systems can be described by a linear system to which is added a virtual input. Section 4 establishes the link with the ADRC framework. Section 5 presents the Generic Linear Extended State Observer that is proposed to estimate, not only the state of the system, but also the virtual input. Some simulation results are shown in section 6 to exhibit the efficiency of the observation scheme. Finally, concluding discussions are given in sections 7 and 8.

2. Problem statement

This paper addresses the state observation problem of unknown nonlinear and time-varying SISO observable (Chen, Bai, & Huang, 2016) systems that obey the three following assumptions.

Assumption 2.1. *The systems of interest are nonlinear, unknown and time-varying, with an input-output dynamics that can be described by an Ordinary Differential Equation (ODE) of order $n > 0$ defined by:*

$$y^{(n)}(t) = f\big(y(t), \ldots, y^{(n-1)}(t), u(t), U'(t), t\big) \tag{1}$$

where

- *the order n is unknown;*
- *the nonlinear and time-varying function f exists but is unknown;*
- *the scalar output $y(t) \in \mathbb{R}$ is the known information provided to the observer. Its n successive derivatives are assumed to be defined but are unknown;*
- *the scalar input $u(t) \in \mathbb{R}$ is the piecewise-continuous known output of the controller that is provided to the observer;*
- *the multidimensional piecewise-continuous disturbance inputs $U'(t) \in \mathbb{R}^\delta$ are assumed unknown. The dimension δ is also unknown. These disturbances can affect the system in any way.*

Assumption 2.2. *The state vector $\mathcal{X} \in \mathbb{R}^n$ of the unknown system defined by (1) is written as*

$$\mathcal{X} = \begin{bmatrix} y & \dot{y} & \cdots & y^{(n-1)} \end{bmatrix}^\mathsf{T}. \tag{2}$$

Assumption 2.3. *The output y and its derivatives $\dot{y}, \ldots, y^{(p-1)}$ with $p > 0$ are assumed necessary to implement the control law of the unknown system. These p components are gathered in the vector*

$$X = \begin{bmatrix} y & \dot{y} & \cdots & y^{(p-1)} \end{bmatrix}^\mathsf{T} \in \mathbb{R}^p \tag{3}$$

that has to be observed, with p being chosen.

With such assumptions, p can be higher, equal or lower than the unknown value n. If $p \leq n$ then the observer will be a reduced-order or a full-order observer of the state $\mathcal{X}$. If $p > n$ then

$$X = \begin{bmatrix} \mathcal{X}^\mathsf{T} & y^{(n)} & \ldots & y^{(p-1)} \end{bmatrix}^\mathsf{T}. \tag{4}$$

In this case, the n state components of $\mathcal{X}$ and $p - n$ additional successive output derivatives will be observed.

3. Equivalent state-space representation

Let us introduce p *a priori* coefficients $a_i \in \mathbb{R}$ and a scalar $b \neq 0$. The nonlinear n-order ODE (1) can be represented by an equivalent linear p-order ODE using the procedure explained below. From (1):

$$y^{(n)} - f(y, \ldots, y^{(n-1)}, u, U', t) = 0 \tag{5}$$

which can be written as

$$\begin{aligned} & y^{(n)} - f(y, \ldots, y^{(n-1)}, u, U', t) \\ & - y^{(p)} + (a_1 y + \ldots + a_p y^{(p-1)} + bu) \\ & + y^{(p)} - (a_1 y + \ldots + a_p y^{(p-1)} + bu) = 0. \end{aligned} \tag{6}$$

Let us define a virtual input $\mathscr{C} \in \mathbb{R}$ by

$$\begin{aligned}\mathscr{C} \triangleq -\frac{1}{b}\Big[\big(y^{(n)} - f(y,\ldots,y^{(n-1)},u,U',t)\big) \\ - y^{(p)} + (a_1 y + \ldots + a_p y^{(p-1)} + bu)\Big]\end{aligned} \tag{7}$$

such that Eq. (6) is equivalent to the following p-order ODE by injecting $\mathscr{C}$ in it:

$$y^{(p)} = a_1 y + \ldots + a_p y^{(p-1)} + bu + b\mathscr{C}. \tag{8}$$

Thanks to (5), it is possible to simplify (7) to

$$\mathscr{C} = -\frac{1}{b}\big[-y^{(p)} + a_1 y + \ldots + a_p y^{(p-1)} + bu\big]. \tag{9}$$

If $p \leq n$, the unknown temporal functions y, $\dot{y}$, …, $y^{(p)}$ in (9) are mathematically defined thanks to (1). If $p > n$, the nonlinear function f has to be $(p-n-1)$-differentiable. Then $y, \ldots, y^{(n)}$ are defined by (1) and the additional unknown temporal functions $y^{(n+1)}$, …, $y^{(p)}$ are mathematically defined by differentiating (1) $p-n-1$ times, leading to:

$$y^{(p)} = \frac{d^{p-n-1}}{dt^{p-n-1}} f\big(y,\ldots,y^{(n-1)},u,U',t\big). \tag{10}$$

As both ODEs (1) and (8) share the same first p initial conditions on $y(t_0),\ldots,y^{(p-1)}(t_0)$, (8) has the *same* input-output behaviour as the unknown nonlinear n-order ODE (1). On a structural point of view, (8) now depends on p known coefficients a_i, a known coefficient b and an unknown virtual input $\mathscr{C}$.

With (3), the equivalent input-output dynamics (8) can be written as a state-space representation using companion form matrices:

$$\left\{\begin{array}{rcl} \dot{X} &=& AX + Bu + B\mathscr{C} \\ y &=& CX \end{array}\right. \tag{11}$$

where $A \in \mathbb{R}^{p\times p}$, $B \in \mathbb{R}^{p\times 1}$ and $C \in \mathbb{R}^{1\times p}$ with

$$A = \begin{bmatrix} 0 & 1 & 0 & 0 & \ldots & 0 \\ 0 & 0 & 1 & 0 & \ldots & 0 \\ 0 & 0 & 0 & 1 & \ldots & 0 \\ & & & \ddots & \ddots & \\ 0 & 0 & 0 & \ldots & 0 & 1 \\ a_1 & a_2 & a_3 & \ldots & a_{p-1} & a_p \end{bmatrix}, \quad B = \begin{bmatrix} 0 \\ 0 \\ 0 \\ \vdots \\ 0 \\ b \end{bmatrix}, \quad C = \begin{bmatrix} 1 & 0 & \ldots & 0 \end{bmatrix}. \tag{12}$$

In (11), the virtual input $\mathscr{C}$ does not have any physical explanation. The additive term $B\mathscr{C}$ is added to the chosen LTI system $AX + Bu$ to obtain the true state derivative $\dot{X}$, and thus the true dynamic of the state X associated to the nonlinear system (1). Like for a process noise, $B\mathscr{C}$ gathers all the differences between the state

evolution of the unknown system (1) and the chosen LTI model. Because of the structure of the LTI system (11), $\mathscr{C}$ is a matched input homogeneous to the control input u .

4. Reduction to the ADRC framework

By setting $X = \left[x_1 \cdots x_p\right]^{\mathsf{T}}$, and using (12), (11) can be put under the following form:

$$\left\{\begin{array}{rcl} \dot{x}_1 &=& x_2, \\ &\vdots& \\ \dot{x}_{p-1} &=& x_p, \\ \dot{x}_p &=& a_1 x_1 + \cdots + a_p x_p + b\,u + b\,\mathscr{C}, \\ y &=& x_1. \end{array}\right. \tag{13}$$

For SISO systems, the classical formulation of ADRC addresses the observation and the control problem of dynamical uncertain systems of order p whose state-space representation is given by (Huang and Xue, 2014):

$$\left\{\begin{array}{rcl} \dot{x}_1 &=& x_2, \\ &\vdots& \\ \dot{x}_{p-1} &=& x_p, \\ \dot{x}_p &=& f(X,d,t) + b(X,t)u, \\ y &=& x_1, \end{array}\right. \tag{14}$$

where d is some unknown external disturbance, $f(X,d,t) \in \mathbb{R}$ and $b(X,t) \in \mathbb{R}$ are some time-varying nonlinear and possibly unknown functions with $b(X,t) \neq 0$. If $b_0 \neq 0$ is chosen to be an estimation of $b(X,t)$, and if the total disturbance, that lumps the model uncertainties and d, is defined as an unknown extended state component x_{p+1}:

$$x_{p+1} \triangleq f(X,d,t) + (b(X,t) - b_0)\,u \tag{15}$$

then Eq. (14) is equivalent to

$$\left\{\begin{array}{rcl} \dot{x}_1 &=& x_2, \\ &\vdots& \\ \dot{x}_{p-1} &=& x_p, \\ \dot{x}_p &=& x_{p+1} + b_0\,u, \\ y &=& x_1 \end{array}\right. \tag{16}$$

that is classically observed using an ESO in the ADRC approach. If all the p coefficients a_i are set to 0 and b is set to b_0, then (13) becomes equivalent to (16) with the total disturbance (unknown extended state x_{p+1}) equal to $b\,\mathscr{C}$. Therefore, the standard SISO state-space formulation of ADRC can be seen as a specific case of the presented methodology.

As opposed to the standard ADRC presented above, in this paper, the p parameters a_i will not be restricted to 0. Sections 6 and 7 provide an example and a discussion on the consequences of having possible non-zero coefficients, including their usefulness and their influence on future control design and generated output noise.

5. Generic Linear Extended State Observer

The state estimation problem of the unknown nonlinear and time-varying system (1) is formulated by the state estimation of its linear equivalent representation (8) combined with the estimation of the unknown virtual input $\mathscr{C} \in \mathbb{R}$. To solve this estimation problem, $\mathscr{C}$ has to be included in some way in an extended state X_e. Such estimation can notably be achieved using a SLESO, a higher-order ESO or a GPI observer. Unlike all of these approaches, the GeLESO proposed in this paper will use the information provided by the p parameters a_i to estimate $\mathscr{C}$ (standard GeLESO) and also the $p-1$ successive derivatives of $\mathscr{C}$ (higher-order GeLESO) in order to improve the efficiency of the estimation of $X \in \mathbb{R}^p$.

5.1. Design of the standard GeLESO

The standard GeLESO is based on the equivalent state-space representation (13). As opposed to SLESO cited above, in which the extended state x_{p+1} represents the total disturbance, the state x_{p+1} in the standard GeLESO includes not only the unknown virtual input $\mathscr{C}$, but also partial information on the linear equivalent representation (8) of the plant:

$$x_{p+1} \triangleq a_1 x_1 + \ldots + a_{p-1} x_{p-1} + b\,\mathscr{C}. \tag{17}$$

Thus x_{p+1} includes all the components of the dynamic of (8) excepted $a_p x_p + b\,u$. Then (13) can be written as:

$$\left\{\begin{array}{rcl} \dot{x}_1 &=& x_2, \\ &\vdots& \\ \dot{x}_{p-1} &=& x_p, \\ \dot{x}_p &=& x_{p+1} + a_p x_p + b\,u, \\ \dot{x}_{p+1} &=& a_1 x_2 + a_2 x_3 + \cdots + a_{p-1} x_p + b\,\dot{\mathscr{C}}, \\ y &=& x_1, \end{array}\right. \tag{18}$$

where $x_1, \ldots, x_{p+1}$ are the $p+1$ components of the extended state X_e. The unknown virtual input $\mathscr{C}$ is deduced from x_{p+1} by:

$$\mathscr{C} = \frac{1}{b}(x_{p+1} - a_1 x_1 - a_2 x_2 - \cdots - a_{p-1} x_{p-1}). \tag{19}$$

The pair (A, C) in (12) being observable thanks to the companion form of matrix A, the state estimation of the system (18) is achieved by a $(p+1)$-order GeLESO designed

as:

$$\left\{\begin{array}{rcl} \dot{z}_1 &=& z_2 + L_1(y - z_1), \\ & \vdots & \\ \dot{z}_{p-1} &=& z_p + L_{p-1}(y - z_1), \\ \dot{z}_p &=& z_{p+1} + a_p z_p + L_p(y - z_1) + bu, \\ \dot{z}_{p+1} &=& a_1 z_2 + \cdots + a_{p-1} z_p + L_{p+1}(y - z_1), \end{array}\right. \tag{20}$$

with $z_{p+1} = a_1 z_1 + a_2 z_2 + \cdots + a_{p-1} z_{p-1} + b\hat{\mathscr{C}}$ and where $z_1, \cdots, z_{p+1}$ are the estimates of states $x_1, \cdots, x_{p+1}$ respectively, and $L_1, \cdots, L_{p+1}$ are the observer gains to be chosen to ensure the stability of (20). Then the virtual input estimation $\hat{\mathscr{C}}$ is given by

$$\hat{\mathscr{C}} = \frac{1}{b}(z_{p+1} - a_1 z_1 - a_2 z_2 - \cdots - a_{p-1} z_{p-1}). \tag{21}$$

As mentioned in (Madoński and Herman, 2013), (Godbole et al., 2013), (Madoński and Herman, 2015), $(p+1)$-order ESO observers implicitly assume that the extended state component x_{p+1} should be slowly time-varying and, thus, its time derivative is ignored. This is the same here for the unknown input $\mathscr{C}$. Thus both SLESO or standard GeLESO may give an insufficient estimation quality if high dynamics are present in x_{p+1}. To improve the state estimation accuracy, higher-order ESO and GPI observers have been developed in which the successive time derivatives of the total disturbance are taken into account. As opposed to aforementioned approaches, in higher-order GeLESO, all the information provided by the p parameters a_i will be used to obtain a better representation of the higher-order dynamics of $\mathscr{C}$ and improve the state estimation.

5.2. Design of the higher-order GeLESO

Let $i > 0$ be the number of extended components in the extended state X_e:

$$X_e = [x_1 \cdots x_p \; x_{p+1} \cdots x_{p+i}]^{\mathsf{T}} \in \mathbb{R}^{p+i}. \tag{22}$$

Like for $\mathscr{C}$ and x_{p+1}, each extended state component x_{p+i} has no physical explanation. They are mathematically introduced to estimate $\mathscr{C}$, $\mathscr{C}^{(1)}$, $\cdots$, $\mathscr{C}^{(i-1)}$ (i terms) with all the $p+i$ components of X_e using some linear combinations explained below.

To proceed with the design of the higher-order GeLESO, the following assumption has to be made:

Assumption 5.1. *$\mathscr{C}$ is a continuous m-differentiable unknown function defined on $\mathbb{R}$, where $m \in \mathbb{N}^*$ with $m \geq i$.*

In (18), the state x_{p+1} was introduced to estimate $\mathscr{C}$. The key idea in the proposed observation scheme is to introduce a state for each derivative of the virtual input to be estimated. This new state is based on the time derivative of the previous one, where all the components are kept, but the last one. For instance, to estimate $\hat{\mathscr{C}}$, the extended component x_{p+2}, has to be introduced by setting $i = 2$. The extended state vector X_e

becomes $X_e = [x_1, \cdots, x_{p+2}]^\mathsf{T}$. According to $\dot{x}_{p+1}$ in Eq. (18), the new state reads as:

$$x_{p+2} \triangleq a_1 x_2 + a_2 x_3 + \cdots + a_{p-2} x_{p-1} + b\dot{\mathscr{C}} \tag{23}$$

because $a_{p-1}x_p$ is not taken into account in it. Thus $\dot{\mathscr{C}}$ now appears in x_{p+2}. It comes the following dynamics on x_1, ..., x_{p+2}:

$$\begin{cases} \dot{x}_k &= x_{k+1}, \quad k = 1, \ldots, p-1, \\ \dot{x}_p &= x_{p+1} + a_p x_p + b\,u, \\ \dot{x}_{p+1} &= x_{p+2} + a_{p-1} x_p, \\ \dot{x}_{p+2} &= a_1 x_3 + a_2 x_4 + \cdots + a_{p-2} x_p + b\ddot{\mathscr{C}}. \end{cases} \tag{24}$$

This dynamics remains an equivalent representation of the uncertain system, but thanks to the extended state components x_{p+1} and x_{p+2}, (24) includes the dynamics of $\mathscr{C}$ and $\dot{\mathscr{C}}$.

For any $i \leq m$, the extended state-space representation of the system (13) will be written in two different ways depending on the value of i, i.e., when $1 \leq i < p$ and when $p \leq i \leq m$.
If $1 \leq i < p$, i.e. as long as the order of the derivative to be estimated is smaller than the size of X, the extended state components are defined by:

$$x_{p+k} \triangleq \sum_{j=1}^{p-k} a_j x_{k+j-1} + b\mathscr{C}^{(k-1)}, \quad k = 2, \cdots, i-1. \tag{25}$$

If $p \leq i \leq m$, i.e. when the order of the derivative to be estimated becomes larger than the size of X, the subsequent extended states only include the previous derivative of $\mathscr{C}$ and read as:

$$x_{p+i} \triangleq b\mathscr{C}^{(i-1)}. \tag{26}$$

According to (25) and (26), the general representation of the system, including the initial system (13) and the extended states, is given by:

$$\begin{cases} \dot{x}_1 &= x_2, \\ &\vdots \\ \dot{x}_p &= x_{p+1} + a_p x_p + bu, \\ \dot{x}_{p+1} &= x_{p+2} + a_{p-1} x_p, \\ &\vdots \\ \dot{x}_{2p-1} &= x_{2p} + a_1 x_p, \\ \dot{x}_{2p} &= b\mathscr{C}^{(p)}, \\ &\vdots \\ \dot{x}_{p+i-1} &= b\mathscr{C}^{(i-1)} \\ \dot{x}_{p+i} &= b\mathscr{C}^{(i)}, \\ y &= x_1. \end{cases} \tag{27}$$

where the first p rows represent the original system (13). The following p rows, i.e.

from $\dot{x}_{p+1}$ to $\dot{x}_{2p-1}$ represent the dynamics of the extended state components defined by (25). The final rows, i.e. from $\dot{x}_{2p}$ to $\dot{x}_{p+i}$ represent the dynamics of the extended states written by (26).

The pair (A, C) in (12) being observable thanks to the companion form of matrix A, the higher-order GeLESO estimating both the states and the extended states, and subsequently the virtual input and its successive derivatives, is built upon (27) and is given by:

$$\left\{\begin{array}{rcl} \dot{z}_1 &=& z_2 + L_1(y - z_1), \\ &\vdots& \\ \dot{z}_p &=& z_{p+1} + a_p z_p + L_p(y - z_1) + bu, \\ \dot{z}_{p+1} &=& z_{p+2} + a_{p-1} z_p + L_{p+1}(y - z_1), \\ &\vdots& \\ \dot{z}_{2p-1} &=& z_{2p} + a_1 z_p + L_{2p-1}(y - z_1), \\ \dot{z}_{2p} &=& z_{2p+1} + L_{2p}(y - z_1), \\ &\vdots& \\ \dot{z}_{p+i-1} &=& z_{p+i} + L_{p+i-1}(y - z_1), \\ \dot{z}_{p+i} &=& L_{p+i}(y - z_1), \end{array}\right. \tag{28}$$

where $z_1, \ldots, z_{p+i}$ are the $p + i$ components of the observer state Z, and where $L_1, \cdots, L_{p+i}$ are the observer gains to be chosen. For implementation purposes, the higher-order GeLESO (28) can be written as:

$$\dot{Z} = (A_e - \mathcal{L}C_e)Z + B_u u + \mathcal{L}y \tag{29}$$

where the matrices $A_e \in \mathbb{R}^{(p+i)\times(p+i)}$, $\mathcal{L} \in \mathbb{R}^{(p+i)\times 1}$, $B_u \in \mathbb{R}^{(p+i)\times 1}$ and $C_e \in \mathbb{R}^{1\times(p+i)}$ are respectively given by:

$$A_e = \begin{bmatrix} 0 & 1 & \cdots & 0 & 0 & 0 & \cdots & 0 & 0 & \cdots & 0 & 0 \\ 0 & 0 & \ddots & & 0 & 0 & \cdots & 0 & 0 & \cdots & 0 & 0 \\ \vdots & \vdots & & \ddots & & & \ddots & \vdots & \vdots & & \vdots & \vdots \\ 0 & 0 & \cdots & 0 & 1 & 0 & & 0 & 0 & \cdots & 0 & 0 \\ 0 & 0 & \cdots & 0 & a_p & 1 & & 0 & 0 & \cdots & 0 & 0 \\ 0 & 0 & \cdots & 0 & a_{p-1} & 0 & \ddots & 0 & 0 & \cdots & 0 & 0 \\ \vdots & \vdots & & & \vdots & & & \ddots & & & \vdots & \vdots \\ 0 & 0 & \cdots & 0 & a_1 & 0 & \cdots & 0 & 1 & & 0 & 0 \\ 0 & 0 & \cdots & 0 & 0 & 0 & \cdots & 0 & 0 & \ddots & 0 & 0 \\ \vdots & \vdots & & & \vdots & \vdots & & \vdots & \vdots & & \ddots & \\ 0 & 0 & \cdots & 0 & 0 & 0 & \cdots & 0 & 0 & \cdots & 0 & 1 \\ 0 & 0 & \cdots & 0 & 0 & 0 & \cdots & 0 & 0 & \cdots & 0 & 0 \end{bmatrix}, \quad \mathcal{L} = \begin{bmatrix} L_1 \\ \vdots \\ L_{p-1} \\ L_p \\ L_{p+1} \\ \vdots \\ L_{p+i} \end{bmatrix}, \tag{30}$$

$$B_u = \begin{bmatrix} 0 & \cdots & 0 & b & 0 & \cdots & 0 \end{bmatrix}^T, \quad C_e = \begin{bmatrix} 1 & 0 & \cdots & 0 \end{bmatrix}$$

One can notice that the p coefficients a_i are included in A_e and gives its specificity. Computing the dynamics of the estimation error by substracting (28) from (27) leads

to:

$$\left\{\begin{array}{rcl} \dot{e}_1 &=& e_2 - L_1 e_1, \\ &\vdots& \\ \dot{e}_p &=& e_{p+1} + a_p e_p - L_p e_1, \\ \dot{e}_{p+1} &=& e_{p+2} + a_{p-1} e_p - L_{p+1} e_1, \\ &\vdots& \\ \dot{e}_{2p-1} &=& e_{2p} + a_1 e_p - L_{2p-1} e_1, \\ \dot{e}_{2p} &=& e_{2p+1} - L_{2p} e_1, \\ &\vdots& \\ \dot{e}_{p+i-1} &=& e_{p+i} - L_{p+i-1} e_1, \\ \dot{e}_{p+i} &=& -L_{p+i} e_1 + b\mathscr{C}^{(i)}, \end{array}\right. \tag{31}$$

which can be put under the more compact form:

$$\dot{E} = (A_e - \mathcal{L}C_e)E + B_e\mathscr{C}^{(i)} \tag{32}$$

and where the matrix $B_e \in \mathbb{R}^{(p+i)\times 1}$ reads as:

$$B_e = \begin{bmatrix} 0 & \cdots & 0 & b \end{bmatrix}^{\mathsf{T}} \tag{33}$$

5.3. Parameterisation of the GeLESO

To ensure the stability of the observation error dynamics (32), the gain matrix $\mathcal{L}$ has to be chosen such that the matrix

$$\mathcal{A} = A_e - \mathcal{L}C_e \ \in \mathbb{R}^{(p+i)\times(p+i)} \tag{34}$$

is Hurwitz. This can be done using pole placement techniques, linear quadratic routines or any other optimisation designs provided that the pair (A_e, C_e) is observable. In this paper, in order to ease the tuning of the observer, a single parameter $\omega_o > 0$ is used as in (Gao, 2003; Zheng, Gao, & Gao, 2007) to specify the components of the gains matrix $\mathcal{L}$:

$$\begin{aligned} \mathcal{L}^{\mathsf{T}} &= [L_1,\ L_2,\ \cdots,\ L_{p+i}] \\ &= [\gamma_1\omega_o,\ \gamma_2\omega_o^2,\ \cdots,\ \gamma_{p+i}\omega_o^{p+i}] \end{aligned} \tag{35}$$

where

$$\gamma_j = \frac{(p+i)!}{j!(p+i-j)!}, \quad \text{with } j = 1, \cdots, p+i. \tag{36}$$

If the p parameters $a_1, \ldots, a_p$ in the matrix A are all set to zero like in ADRC, then using the same proof as the one in (Zheng et al., 2007), it can be easily shown that the $p+i$ observer poles are placed in $-\omega_o$ and that $\mathcal{A}$ is Hurwitz.
If any parameters $a_1, \ldots, a_p$ are chosen different from zero, then the gains $\mathcal{L}'$ that are placing the poles in $-\omega_o$ are close to the gains $\mathcal{L}$ given by Eq. (35)-(36) provided that the bandwidth ω_o is chosen large enough. In this case, the Hurwitz property has not

been proven for $A_e - \mathcal{L}C_e$ with any ω_o and a_i. Thus, in the following, it will be assumed that it is verified that $\mathcal{A}$ is Hurwitz for the chosen values of ω_o and $a_1, \ldots, a_p$.

5.4. Convergence of the GeLESO

In this section, the convergence analysis of the proposed GeLESO is presented. It is shown that, in some cases depending on the order of the derivatives of the virtual input $\mathscr{C}$, the asymptotic convergence of each component E_j of the estimation error E can be achieved. For the cases where the asymptotic convergence is not achieved, it is shown that the estimation error is bounded, and the bound is provided. This result is achieved provided that the following assumption is verified.

Assumption 5.2. *$\mathscr{C}^{(i)}$ is bounded by some positive constant β, i.e. $\forall i \in \mathbb{N}^*$ with $1 \leq i \leq m$, $\exists \beta \in \mathbb{R}^+$ such that $|\mathscr{C}^{(i)}| < \beta$.*

The different cases are summed up in the following theorem:

Theorem 5.3. *Provided that assumptions 5.1 and 5.2 are satisfied, $\forall\, p$, order of the non physical chosen LTI model, $\forall\, m$, number of times that the virtual input $\mathscr{C}$ is differentiated, $\forall\, i$, number of times that the state of the initial system* (13) *is extended, and $\forall\, j = 1, \cdots, p+i$, the following statements are verified:*

$\mathbb{S}1$: If $i = m$ and $\mathscr{C}^{(m)} = 0$, then $\lim\limits_{t \to +\infty} |E_j(t)| = 0$.

$\mathbb{S}2$: If $i = m$, and $\mathscr{C}^{(m)} \neq 0$, then $\exists\ \alpha_j \in \mathbb{R}^+$ such that $\lim\limits_{t \to +\infty} |E_j(t)| \leq \alpha_j$.

$\mathbb{S}3$: If $i < m$ and $\mathscr{C}^{(i)} = 0$, then $\lim\limits_{t \to +\infty} |E_j(t)| = 0$.

$\mathbb{S}4$: If $i < m$, $\forall\ \mathscr{C}^{(i)} \neq 0$, then $\exists\ \zeta_j \in \mathbb{R}^+$ such that $\lim\limits_{t \to +\infty} |E_j(t)| \leq \zeta_j$.

Proof. See Appendix A. □

5.5. Influence of the GeLESO order on the estimation error

In this section, it will be shown that the more the order of the GeLESO increases, the more the estimation error E of the extended state X_e decreases, provided that the following assumption is true.

Assumption 5.4. *The parameter ω_o is chosen such that $\omega_o > \omega_{max}$, with ω_{max} defined in* (B7) *in the proof of Theorem 5.5 in Appendix B.*

Theorem 5.5. *Provided that assumption 5.4 is satisfied, let us consider two GeLESO designed with different orders, but the same ω_o. The one of order $p+i$ will be noted GeLESO$|_i$ and the one of order $p+k$ will be noted GeLESO$|_k$, $\forall\, i,\ k \in \mathbb{N}^*$ with $i < k$.*

We denote by $|E_j(t)|_i$ and $|E_j(t)|_k$ the estimation error of the component j associated to GeLESO$|_i$ and GeLESO$|_k$ respectively, where $j = 1, \cdots, p+i$. In the case of statements $\mathbb{S}1$ and $\mathbb{S}3$:

$$\lim_{t\to+\infty} |E_j(t)|_k = \lim_{t\to+\infty} |E_j(t)|_i = 0. \tag{37}$$

In the case of statements $\mathbb{S}2$ and $\mathbb{S}4$:

$$\lim_{t\to+\infty} |E_j(t)|_k < \lim_{t\to+\infty} |E_j(t)|_i. \tag{38}$$

Proof. See Appendix B.

□

6. Illustrative example

In order to illustrate its efficiency, higher-order GeLESO is compared to GPI observers (Luviano-Juárez et al., 2010; Sira-Ramírez et al., 2017) and higher-order ESO (Godbole et al., 2013; Madoński and Herman, 2015) that have a similar internal structure. The proposed approach is applied on a Genesio-Tesi Chaotic system studied in (Luviano-Juárez et al., 2010), on which a varying disturbance is added to make the state estimation more complex. A white measurement noise will also be added in a second time. The unknown dynamics of $\mathcal{X} = [x_1\, x_2\, x_3]^\mathsf{T}$ is given by:

$$\begin{cases} \dot{x}_1 &= x_2, \\ \dot{x}_2 &= x_3, \\ \dot{x}_3 &= -6x_1 - 2.92x_2 - 1.2x_3 + x_1^2 + d(t), \\ y &= x_1, \end{cases} \tag{39}$$

where y is the output of the system and $d(t) = \sin(2\,t)$ represents a varying disturbance that is always affecting the system. The initial conditions of (39) are kept the same as in (Luviano-Juárez et al., 2010), i.e. $x_1(0) = -1$, $x_2(0) = -2$ and $x_3(0) = 1$.

In order to validate the equivalent state-space representation (11), one can choose any value $p > 0$. A full-order observer ($p = 3$) is here chosen to test in simulation the estimation of all the state components of $\mathcal{X}$. The same way as in (12), the state matrix A and the input matrix B are:

$$A = \begin{bmatrix} 0 & 1 & 0 \\ 0 & 0 & 1 \\ a_1 & a_2 & a_3 \end{bmatrix}, \quad B = \begin{bmatrix} 0 \\ 0 \\ b \end{bmatrix}. \tag{40}$$

The coefficient b will affect the value of $\mathscr{C}$. It is taken equal to 1. In test 1, the coefficients a_i are chosen to have no physical meaning: $a_1 = -8$, $a_2 = -8$, $a_3 = -0.8$. In test 2, the coefficients are specifically chosen to be equal to the linear dynamics of the system (39) (that is just for simulation purposes as this dynamics should normally be unknown), i.e. $a_1 = -6$, $a_2 = -2.92$, $a_3 = -1.2$.

We propose to introduce 5 extended states ($i = 5$) as what is done in (Luviano-Juárez et al., 2010). Then, the higher-order GeLESO, GPI observer and higher-order

ESO estimation dynamics are given by:

GeLESO	GPI observer	Higher-order ESO
$\dot{z}_1 = z_2 + L_1 e_1$	$\dot{z}_1 = z_2 + L_1 e_1$	$\dot{z}_1 = z_2 + L_1 e_1$
$\dot{z}_2 = z_3 + L_2 e_1$	$\dot{z}_2 = z_3 + L_2 e_1$	$\dot{z}_2 = z_3 + L_2 e_1$
$\dot{z}_3 = z_4 + a_3 z_3 + L_3 e_1$	$\dot{z}_3 = \rho_1 + L_3 e_1$	$\dot{z}_3 = z_4 + L_3 e_1$
$\dot{z}_4 = z_5 + a_2 z_3 + L_4 e_1$	$\dot{\rho}_1 = \rho_2 + L_4 e_1$	$\dot{z}_4 = z_5 + L_4 e_1$
$\dot{z}_5 = z_6 + a_1 z_3 + L_5 e_1$	$\dot{\rho}_2 = \rho_3 + L_5 e_1$	$\dot{z}_5 = z_6 + L_5 e_1$
$\dot{z}_6 = z_7 + L_6 e_1$	$\dot{\rho}_3 = \rho_4 + L_6 e_1$	$\dot{z}_6 = z_7 + L_6 e_1$
$\dot{z}_7 = z_8 + L_7 e_1$	$\dot{\rho}_4 = \rho_5 + L_7 e_1$	$\dot{z}_7 = z_8 + L_7 e_1$
$\dot{z}_8 = L_8 e_1$	$\dot{\rho}_5 = L_8 e_1$	$\dot{z}_8 = L_8 e_1$

where $e_1 = y - z_1$. The ρ_i are the extra states in the GPI observer (Luviano-Juárez et al., 2010). For all three observers, initial conditions are null and the observer gains $L_1, \ldots, L_8$ are calculated using (35), where $\omega_o = 5$. One can see that the GPI observer and the higher-order ESO have the same internal structure and will provide the same estimation results. The observer gains for the three observation strategies are all the same and given below:

$$\mathcal{L} = [\,40 \quad 700 \quad 7000 \quad 43750 \quad 175000 \quad 437500 \quad 625000 \quad 390625\,]^{\mathsf{T}}.$$

Figure 1 illustrates that (39) (black curve) gives the same temporal behaviour $y(t)$ as (11) (blue curve). The virtual input $\mathscr{C}$ plotted in red is computed using (9) with the coefficients a_i defined in test 1. Its estimation $\hat{\mathscr{C}}$ using (21) is the dashed blue line. Note that the peak in the transient phase of the estimation is cropped.

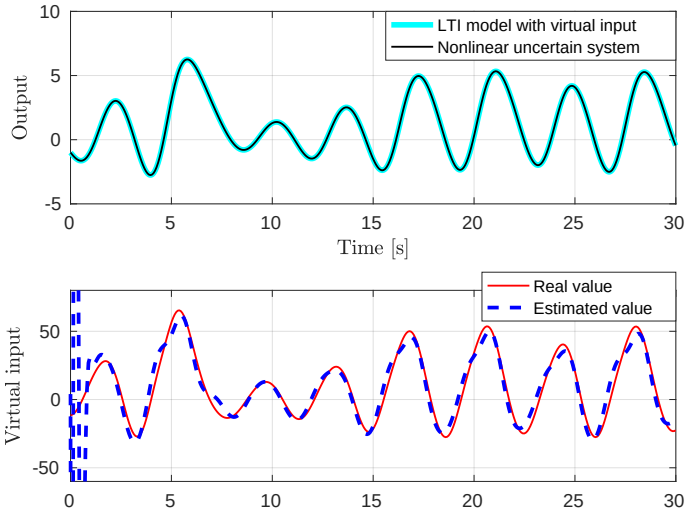

Figure 1. Evolution of the output y and virtual input $\mathscr{C}$

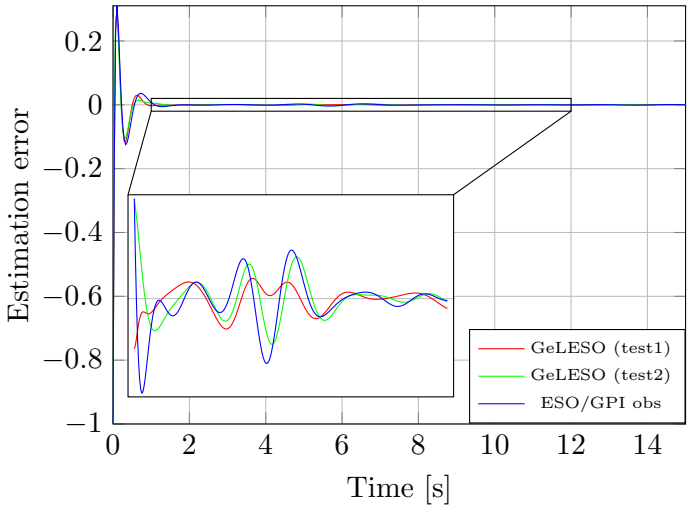

Figure 2. Estimation errors of component x_1

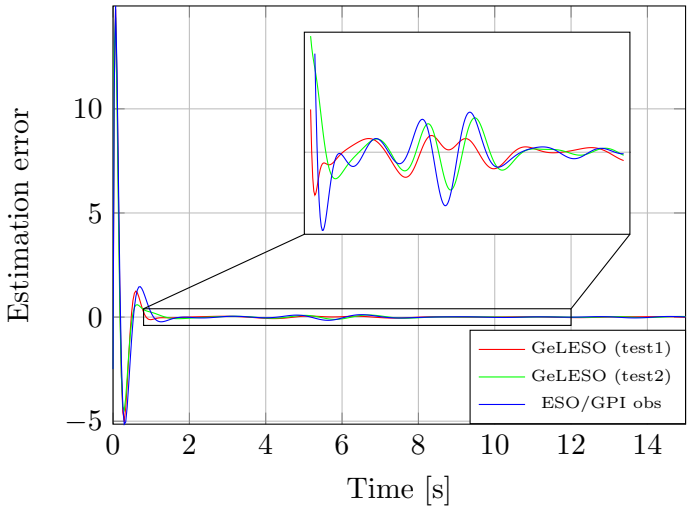

Figure 3. Estimation errors of component x_2

6.1. Estimation error analysis

Figures 2, 3 and 4 show the estimation errors for the state components x_1, x_2 and x_3 respectively. Table 1 gives, for these three x_j, the magnitude WE_j of the upper bound of the error on a finite-time window using the higher-order GeLESO and higher-order ESO/GPI observers designed above. WE_j is defined as

$$\mathrm{WE}_j = \sup_{t\in[t_1,t_1+\tau]} |E_j(t)| \tag{41}$$

with t_1 chosen much larger than the response time of the observer and E defined by (32). In table 1, the results are given for $t_1 = 20$ s and $\tau = 10$ s. That table shows an improvement of the accuracy of state observation for the proposed higher-order GeLESO with respect to the higher-order ESO/GPI observers when all observers have the same gains. Table 2 shows the same results for only 4 extended states ($i = 4$).

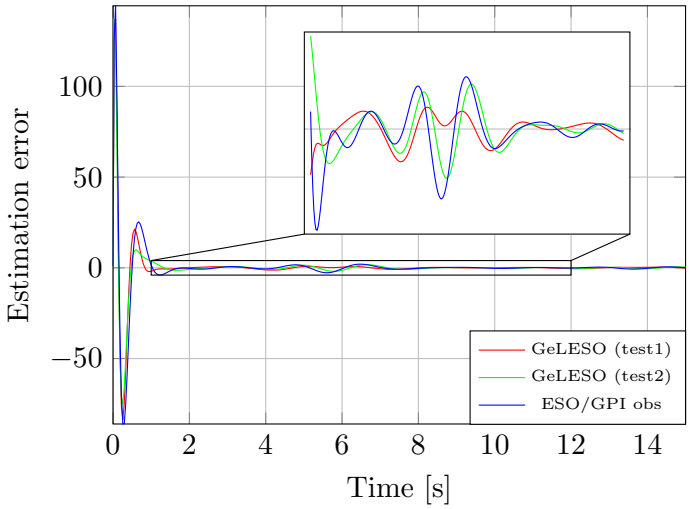

Figure 4. Estimation errors of component x_3

One can see by comparing the two tables that GeLESO in test 1 remains close or more efficient with only 4 extended states than the higher-order ESO/GPI observers with 5 extended states.

Table 1. WE_j associated to x_j for $i = 5$

	ESO/GPI obs	GeLESO	
		a_i (test1)	a_i (test2)
x_1	0.0032	0.0017	0.0023
x_2	0.1304	0.0700	0.0918
x_3	2.2785	1.1717	1.6047

Table 2. WE_j associated to x_j for $i = 4$

	ESO/GPI obs	GeLESO	
		a_i (test1)	a_i (test2)
x_1	0.0060	0.0035	0.0035
x_2	0.2107	0.1235	0.1225
x_3	3.1580	1.8509	1.8360

In order to investigate the influence of the parameters a_i on the estimation error for the state components, Monte-Carlo simulations have been performed to provide a statistical analysis. This analysis was done by picking 1000 random sets of parameters a_i with a 100 % variation around the nominal values of test 1. The values taken by the random parameters are given by uniform distributions. The results of this analysis are given in the form of histograms presented in figures 5, 6 and 7. On these histograms, the estimation error of the higher-order ESO / GPI observer is represented by the dashed vertical red line.

That can be explained by the root locus of the GeLESO that is also provided for all the state components z_1 to z_8 shown in Figure 8. From this figure, one can see that the poles of the observer are not all placed in $-\omega_o$ as mentioned in section 5.3. Some poles are faster and some others are slower and thus change the dynamics of

the observation compared to the higher-order ESO / GPI observer.

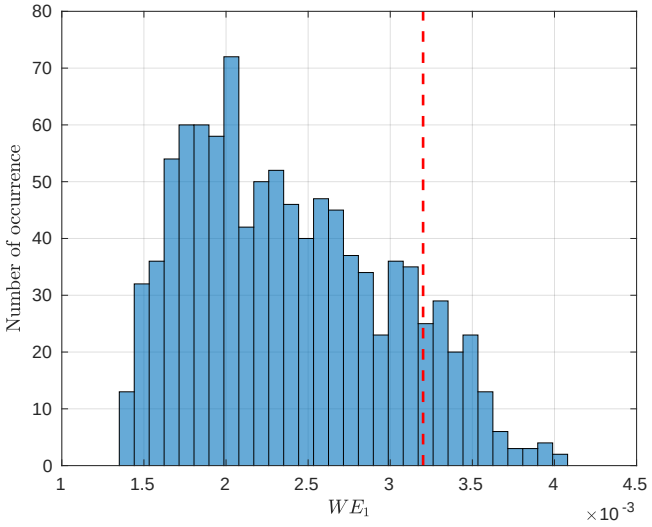

Figure 5. Distribution of the estimation error WE_1 of state component x_1

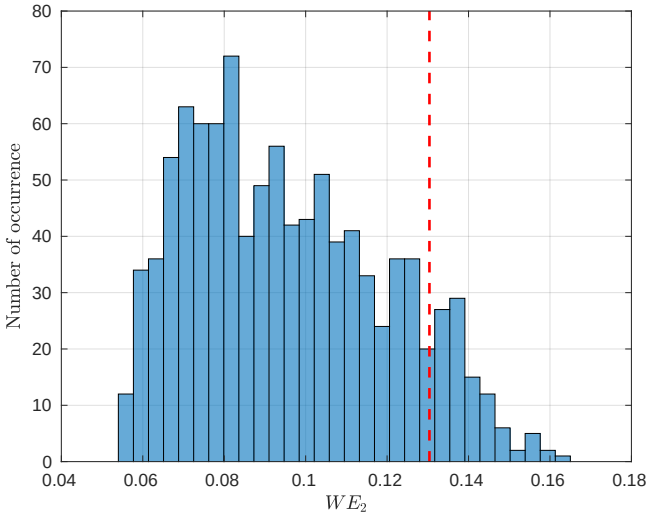

Figure 6. Distribution of the estimation error WE_2 of state component x_2

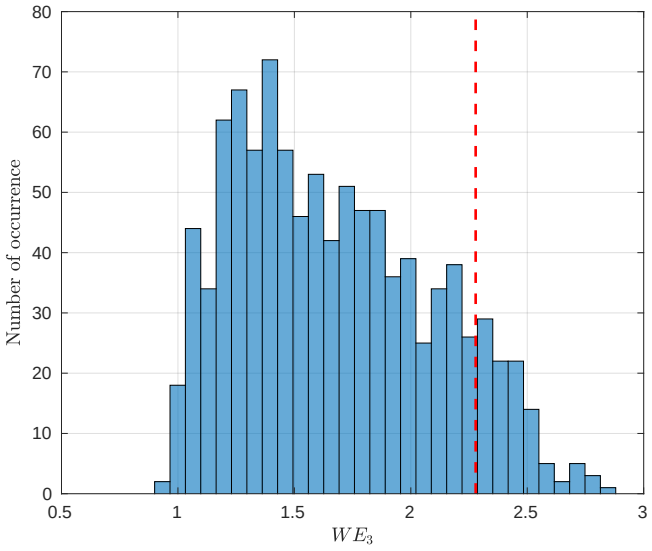

Figure 7. Distribution of the estimation error WE_3 of state component x_3

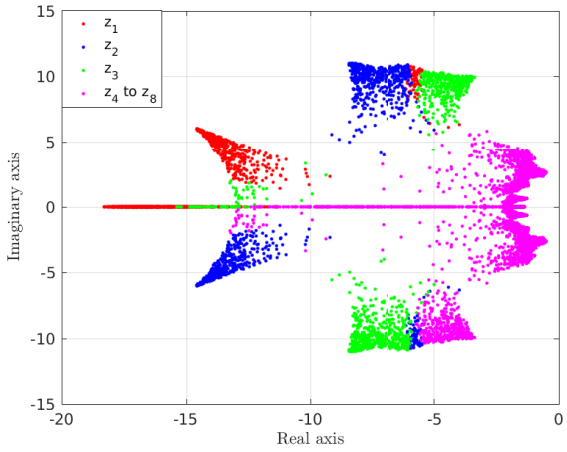

Figure 8. Root locus of the observer of order $p + i = 8$

6.2. Noise analysis

To study the sensitivity of the GeLESO to measurement noise, a white noise $v(t)$ is added to the output y and the measured output $y_m = y + v$ is fed into each observers. The infinite variance and zero-mean white Gaussian noise v is chosen to have a Power Spectral Density p_v equal to 10^{-6}. Each observer's statistical behaviour remains the same if v is replaced by a band-limited white Gaussian noise v' having the same PSD up to a cutoff frequency $\omega_c >> \omega_0$ and a finite variance R that can be simulated. In the simulation, ω_c is set to $\pi.10^4$ rad/s. The variance $R = p_v \dfrac{\omega_c}{2\pi}$ is then equal to 0.005. Figure 9 shows y, y_m and the estimation z_1 provided by the higher-order GeLESO (test 1) with these settings. As each observer is linear, it is characterised by a Gaussian random extended state $\underline{Z}$ given by:

$$\underline{Z} = Z + \tilde{\underline{Z}} \tag{42}$$

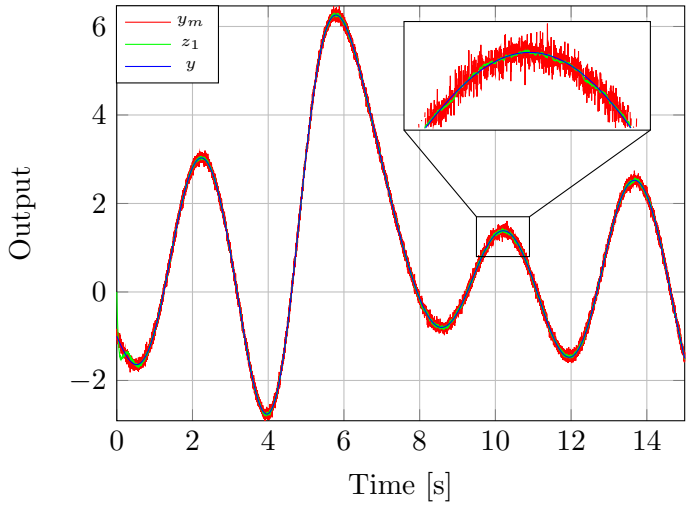

Figure 9. Evolution of output y, measured output y_m and output estimation z_1

with Z representing the deterministic behaviour of the observer previously determined for y (with $v = 0$) and $\underline{\tilde{Z}}$ representing the zero-mean Gaussian behaviour associated to v (with $y = 0$). The covariance matrix $P(t) = E\left[\underline{\tilde{Z}}(t)\underline{\tilde{Z}}(t)^{\mathsf{T}}\right]$ has a steady-state value P given by the solution of the continuous-time Lyapunov equation:

$$(A_e - \mathcal{L}C)P + P(A_e - \mathcal{L}C)^T + \mathcal{L}p_v\mathcal{L}^T = 0 \tag{43}$$

with $\mathcal{L}$ given by (35). The diagonal components of P give the variance of the asymptotic stationary noise present on each component of the state observation $\underline{Z}$. Figures 10, 11 and 12 show the effect of ω_o on the observer noise ratio

$$NR_j = \frac{\sqrt{P_{jj}}}{\sqrt{R}} \tag{44}$$

that expresses how the measurement noise v' is amplified by the observer on the j^{th} state component. This noise ratio is an increasing function of ω_o and it is a little smaller on the GeLESO than on the higher-order ESO/GPI observers. For $\omega_0 = 5$, the measurement noise is attenuated for z_1 (which is verified in Fig. 9), slightly amplified in z_2 and much more amplified in z_3. More generally, the higher is j and the bigger is the observer noise ratio for z_j.

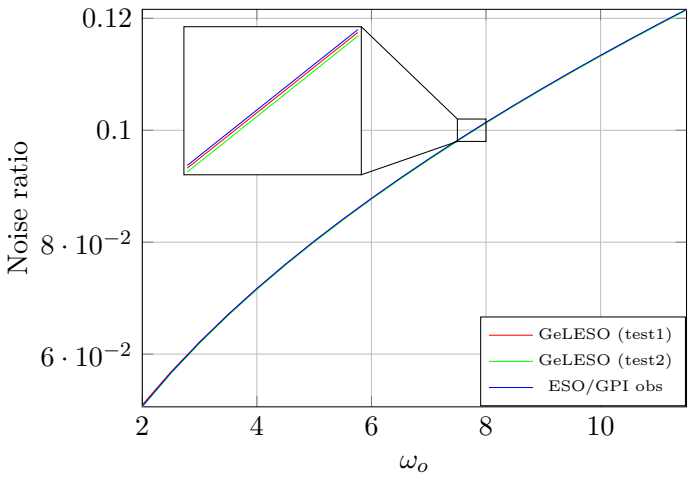

Figure 10. Effect of ω_o on the observer noise ratio for the estimation of x_1

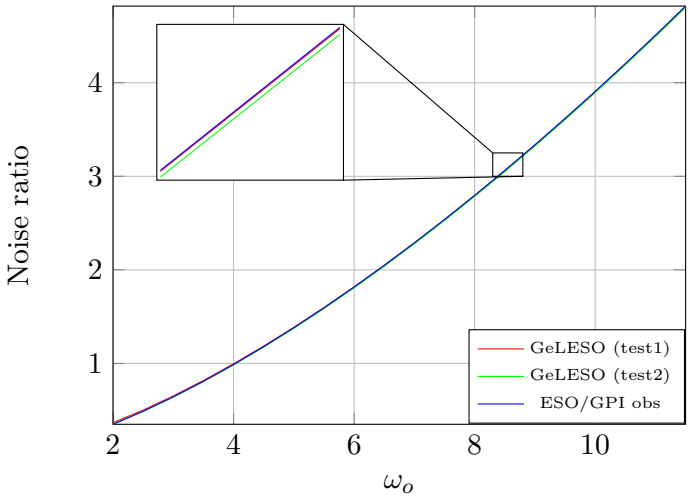

Figure 11. Effect of ω_o on the observer noise ratio for the estimation of x_2

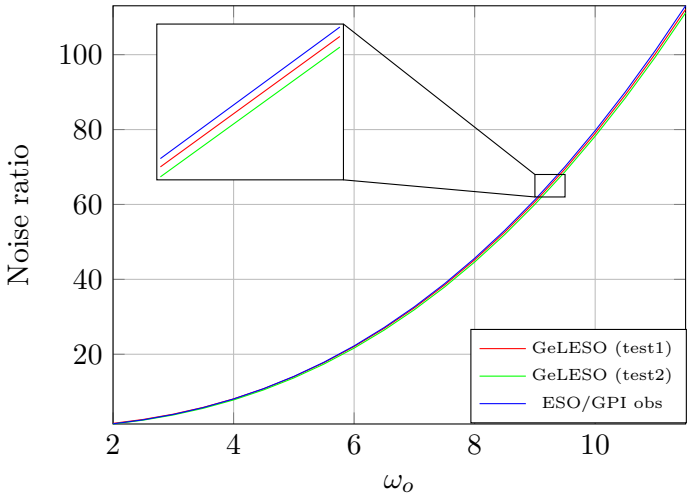

Figure 12. Effect of ω_o on the observer noise ratio for the estimation of x_3

Figure 13 illustrates how the number i of extended states influences the GeLESO noise ratio for z_1 in test 1. It can be seen that, for any ω_o, the higher the parameter i, the stronger is the noise amplification in the estimation of state x_1. Finally, the histogram presented in figure 14 shows the distribution of the noise ratio NR_1 for the state component z_1 and for the same statistical analysis as the one provided in the previous section. The limited statistical range of this distribution illustrates that the estimation noise of the GeLESO has a low sensitivity to different sets of parameters a_i. That can be explained from Figure 8 where the poles corresponding to the extended state components are among the slowest ones, hence having little influence on the noise.

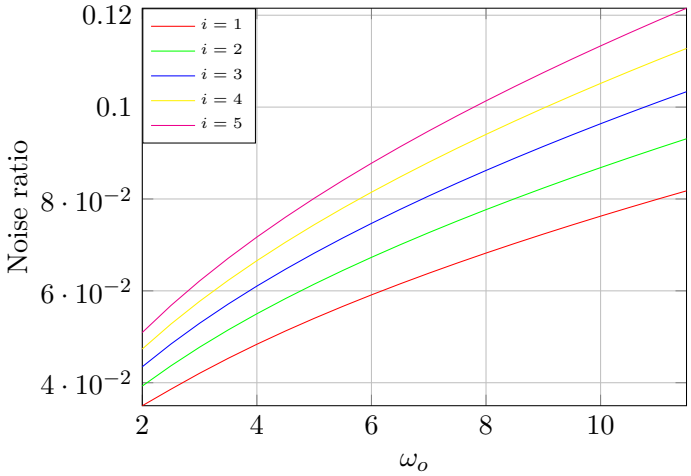

Figure 13. Effect of the number of extended states i on the GeLESO noise ratio for the estimation of x_1 in test 1

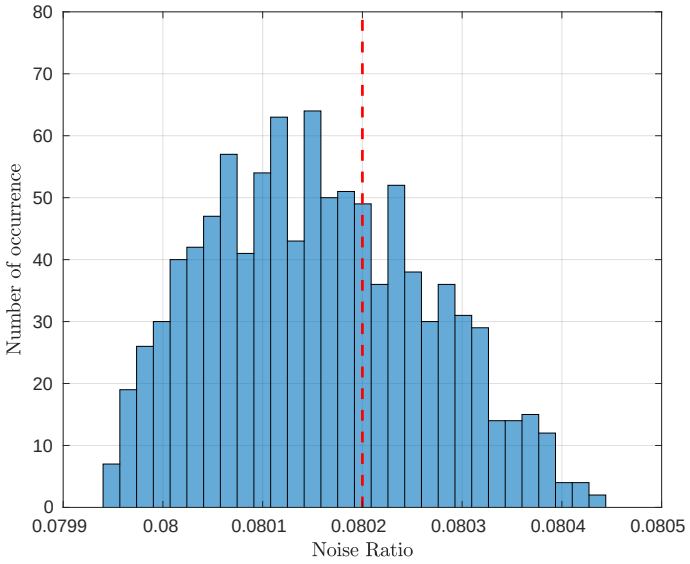

Figure 14. Distribution of the noise ratio (44) for state component z_1 with $\omega_o = 5$

7. Discussion and perspectives

Having possible non-zero coefficients a_i (as opposed to common ADRC where these coefficients are null) asks the question of their choice and future control design. Some preliminary elements for future studies on this issue are given in this section. These elements express that the coefficients choice and the control design are both related.

A possible control scheme for the unknown nonlinear system (1) may consist in decomposing u into two parts $u = u_1 + u_2$. Like in ADRC, an approximate global linearisation of (1) is firstly performed. It is here achieved by canceling the virtual input $\mathscr{C}$ with a negative feedback $u_1 = -\hat{\mathscr{C}} = -\varphi(Z)$, that is the first step of the Virtual Input Rejection Control (VIRCO) scheme introduced in this section. This preliminary control u_1 uses the estimation Z provided by the GeLESO and the linear operator φ described by (21). Using this specific feedback u_1, the equivalent dynamical behaviour (11) becomes

$$\left\{ \begin{array}{rcl} \dot{X} & = & AX + Bu_2 + \varepsilon \\ y & = & CX \end{array} \right. \tag{45}$$

with ε being a nonlinear residual that depends on the estimation quality of the GeLESO that is defined by:

$$\varepsilon = B(\mathscr{C} - \hat{\mathscr{C}}) \tag{46}$$

This residual cannot be estimated because all the *a priori* available information a_i and b has been used to provide $\hat{\mathscr{C}}$. Thus, ε acts as an unknown disturbance and its effect on y has to be minimised to obtain a closed-loop dynamic that is as close as possible to the associated LTI model. As the residual ε depends on the a_i and b that gives $\hat{\mathscr{C}}$, these coefficients have to be chosen in a way that minimises $|\varepsilon|$. To achieve this, some online optimisation strategies are possible. To introduce the criteria to minimise, let

us consider the two following state dynamics:

$$\dot{X} = AX + Bu + B\mathscr{C}, \tag{47}$$

$$\dot{X}' = AX' + Bu + B\hat{\mathscr{C}} \tag{48}$$

$$= AX' + Bu_2. \tag{49}$$

Equation (47) is the same as (11) which gives the state X of system (1). Equation (48) is associated to a new state X' for which the virtual input $\mathscr{C}$ has been substituted to $\hat{\mathscr{C}}$. As shown by (49) it is also the dynamics of the chosen LTI model with $u = u_1 + u_2 = -\hat{\mathscr{C}} + u_2$. As u and $\hat{\mathscr{C}}$ are known, X' can be computed online and used in the minimisation criteria. By difference between (47) and (48), it comes

$$\dot{X} - \dot{X}' = A(X - X') + \varepsilon.$$

If A is Hurwitz, the closer is X to X' and the smaller is $|\varepsilon|$. Hence, the optimisation process of the coefficients a_i that minimises $|\varepsilon|$ can be associated to the minimisation of the difference $|X - X'|$. Nevertheless, in practice, the state X is unknown. Thus it has to be replaced by its estimation $\hat{X}$ given by the GeLESO, with an error characterized by (32). Theorem 5.3 also states that the limit of this error can be bounded or null. Therefore, the parameters a_i will adjust to minimise the criteria $|\hat{X} - X'|$, that will in return minimise $|\varepsilon|$. Such an approach would fit into the framework of adaptive observers.

If $|\varepsilon| = 0$ is achieved, (45) becomes equivalent to

$$\left\{ \begin{array}{rcl} \dot{X} & = & AX + Bu_2 \\ y & = & CX. \end{array} \right. \tag{50}$$

Such representation is richer than in the conventional ADRC framework and its associated p poles can then be placed easily with a secondary control $u_2 = -KZ$. Having more poles thanks to the choice of p may bring more possibilities to adjust finely the control. The observation noise in $\hat{\mathscr{C}}$ and Z will add some noise on the control input u of the system. Such noise may be prejudicial (mechanical wear of the actuators for instance) and should be avoided with an appropriate choice of a_i and b. This input noise on u is then filtered by the system whose dynamical behaviour is now close to (50) and provides a noise on y. Thus, using appropriate coefficients a_i to have a low pass behaviour, the noise generated on y can be limited, which is mandatory to reach high control performance. Finally, the final goal of such control scheme is the achievement of a pole placement of a linear virtual system (50) that has substituted the unknown system (1). This asks the question of the feasibility of the control u in term of stability, bounds, etc. This issue constitutes clearly a perspective to this work.

8. Conclusion

The generic methodology proposed in this paper can be applied to a given class of observable unknown nonlinear and time-varying SISO systems with unknown order,

structure and disturbances. The proposed methodology can be seen as a first step towards a generalisation of the ADRC framework. To this end, the state observation of the unknown SISO nonlinear systems is transformed into the state observation of an arbitrary known observable LTI systems and an unknown virtual input. This observation is performed with a Generic Linear Extended State Observer that is introduced in the paper. This specific observer uses the parameters present in the chosen LTI system to introduce higher-order state components that take into account the unknown virtual input and its successive derivatives. A mathematical proof that demonstrates the reason of designing higher-order GeLESO to improve the accuracy of the proposed observer is also given. Numerical simulations based on a Genesio-Tesi Chaotic system affected by a varying disturbance show that the proposed observer gives better results than classical higher order ESO / GPI observers provided that the observer coefficients are well chosen.

Acknowledgment

This work has been supported by the EIPHI Graduate school (contract "ANR-17-EURE-0002").

References

Astolfi Daniele (2016). *Observers and Robust Output Regulation for Nonlinear Systems*. PSL Research University.

Astolfi Daniele, Marconi Lorenzo, Praly Laurent and Teel Andrew R. (2018). Low-Power Peaking-Free High-Gain Observers. *Automatica*, *98*, 169–179.

Chen Sen, Bai Wenyan and Huang Yi (2016). ADRC for Systems with Unobservable and Unmatched Uncertainty. Proceedings of the 35th Chinese Control Conference, Chengdu, China.

Dong Yali, Wang Hui and Wang Yangang (2013). Design of Observers for Nonlinear Systems with H_∞ Performance Analysis. *Mathematical Methods in the Applied Sciences*, *37*(5), 718–725.

Feng Guang, Liu Yan-Fei and Huang Lipei (2004). A New Robust Algorithm to Improve the Dynamic Performance on the Speed Control of Induction Motor Drive. *IEEE Transactions on Power Electronics*, *19*(6), 1614–1627.

Freidovich Leonid B. and Khalil Hassan K. (2008). Performance Recovery of Feedback-Linearization-Based Designs. *IEEE Transactions on Automatic Control*, *53*(10), 2324–2334.

Gao Zhiqiang, Huang Yi and Han Jingqing (2001). An Alternative Paradigm for Control System Design. Proceedings of the 40th Conference on Decision and Control, Orlando, FL, USA.

Gao Zhiqiang (2003). Scaling and Bandwidth-Parameterization Based Controller Tuning. Proceedings of the American Control Conference, Denver, CO, USA.

Gao Zhiqiang (2006). Active Disturbance Rejection Control: A Paradigm Shift in Feedback Control System Design. Proceedings of the American Control Conference, Minneapolis, MN, USA.

Gauthier Jean-Paul, Hammouri Hassan and Othman Sami (1992). A Simple Observer for Nonlinear Systems - Applications to Bioreactors. *IEEE Transactions on Automatic Control*, *37*(6), 875–880.

Godbole Ashwini A., Kolhe Jaywant P. and Talole Sanjay E. (2013). Performance Analysis of Generalized Extended State Observer in Tackling Sinusoidal Disturbances. *IEEE Transactions on Control Systems Technology*, *21*(6), 2212–2223.

Guo Bao-Zhu and Zhao Zhi-Liang (2016). *Active Disturbance Rejection Control for Nonlinear Systems: An Introduction*. Wiley.

Han Jingqing Q. (1995). The Extended State Observer for a Class of Uncertain Systems. *Control and Decision*, *10*(1), 85–88.

Huang Yi and Xue Wenchao (2014). Active Disturbance Rejection Control: Methodology and Theoretical Analysis. *ISA Transactions*, *53*(4), 963–976.

Julier Simon J. and Uhlmann Jeffrey K. (1997). A New Extension of the Kalman Filter to Nonlinear Systems. Proceedings of AeroSense: 11th International Symposium on Aerospace / Defense Sensing, Simulations and Controls, Orlando, FL, USA.

Kalman Rudolf E. (1960). A New Approach to Linear Filtering and Prediction Problems. *Journal of Basic Engineering*, *82*(1), 35–45.

Khalil Hassan K. and Praly Laurent (2013). High-Gain Observers in Nonlinear Feedback Control. *International Journal of Robust and Nonlinear Control*, *24*(6), 993–1015.

Kim Kyung-Soo, Rew Keun-Ho and Kim Soohyun (2010). Disturbance Observer for Estimating Higher Order Disturbances in Time Series Expansion. *IEEE Transactions on Automatic Control*, *55*(8), 1905–1911.

Krener Arthur J. and Isidori Alberto (1983). Linearization by Output Injection and Nonlinear Observers. *Systems & Control Letters*, *3*(1), 47–52.

Li Shihua, Yang Jun, Chen Wen-Hua and Chen Xisong (2012). Generalized Extended State Observer Based Control for Systems with Mismatched Uncertainties. *IEEE Transactions on Industrial Electronics*, *59*(12), 4792–4802.

Li Shihua, Yang Jun, Chen Wen-Hua and Chen Xisong (2014). *Disturbance Observer-Based Control - Methods and Applications*. CRC Press.

Luenberger David G. (1964). Observing the State of a Linear System. *IEEE Transactions on Military Electronics*, *8*(2), 74–80.

Luviano-Juárez Alberto, Cortés-Romero John and Sira-RamÍrez Hebertt (2010). Synchronization of Chaotic Oscillators by Means of Generalized Proportional Integral Observers. *International Journal of Bifurcation and Chaos*, *20*(5), 1509–1517.

Madoński Rafal and Herman Przemyslaw (2013). On the Usefulness of Higher-Order Disturbance Observers in Real Control Scenarios based on Perturbation Estimation and Mitigation. Proceedings of the 9th International Workshop on Robot Motion and Control, Kuslin, Poland.

Madoński Rafal and Herman Przemyslaw (2015). Survey on Methods of Increasing the Efficiency of Extended State Disturbance Observers. *ISA Transactions*, *56*, 18–27.

Marconi Lorenzo, Praly Laurent and Isidori Alberto (2007). Output Stabilization via Nonlinear Luenberger Observers. *SIAM Journal on Control and Optimization*, *45*(6), 2277–2298.

Sira-Ramírez Hebertt, Luviano-Juárez Alberto, Ramírez-Neria Mario and Zurita-Bustamante Eric William (2017). *Active Disturbance Rejection Control of Dynamic Systems - A Flatness Based Approach*. Butterworth-Heinemann.

Suykens Johan A. K., Vandewalle Joos P. L. and De Moor Bart L. R. (1996). *Artificial Neural Networks for Modelling and Control of Non-Linear Systems*. Springer.

Talole Sanjay E., Kolhe Jayawant P. and Phadke Srivijay B. (2010). Extended-State-Observer-Based Control of Flexible-Joint System with Experimental Validation. *IEEE Transactions on Industrial Electronics*, *57*(4), 1411–1419.

Wang Junxiao, Li Shihua, Yang Jun, Wu Bin and Li Qi (2015). Extended State Observer-Based Sliding Mode Control for PWM-Based DC–DC Buck Power Converter Systems with Mismatched Disturbances. *IET Control Theory & Applications*, *9*(4), 579–586.

Xia Yuanqing, Zhu Zheng, Fu Mengyin and Wang Shuo (2011). Attitude Tracking of Rigid Spacecraft with Bounded Disturbances. *IEEE Transactions on Industrial Electronics*, *58*(2), 647–659.

Yang Xiaoxia and Huang Yi (2009). Capabilities of Extended State Observer for Estimating Uncertainties. Proceedings of the American Control Conference, Saint-Louis, MO, USA.

Zeitz Michael (1987). The Extended Luenberger Observer for Nonlinear Systems. *Systems & Control Letters*, *9*(2), 149–156.

Zheng Qing, Gao Linda Q. and Gao Zhiqiang (2007). On Stability Analysis of Active Disturbance Rejection Control for Nonlinear Time-Varying Plants with Unknown Dynamics. Proceedings of the 46th Conference on Decision and Control, New Orleans, LA, USA.

Appendix A. Proof of Theorem 5.3

Statements $\mathbb{S}1$ and $\mathbb{S}3$ mean that the higher-order GeLESO estimates the state X, the virtual input $\mathscr{C}$ and its successive derivatives until $\mathscr{C}^{(m-1)}$ without steady-state error.
Statements $\mathbb{S}2$ and $\mathbb{S}4$ mean that the higher-order GeLESO estimates the state X, the virtual input $\mathscr{C}$ and its successive derivatives until $\mathscr{C}^{(m-1)}$ with a bounded error.

A.1. Proof of statement $\mathbb{S}1$

If $i = m$ and $\mathscr{C}^{(m)} = 0$, then $\mathscr{C}^{(i)} = 0$. In that case, the dynamics of the estimation error (32) can be written as:

$$\dot{E} = (A_e - \mathcal{L}C_e)E = \mathcal{A}E \tag{A1}$$

whose solution is: $E(t) = e^{\mathcal{A}t}E(0)$.
Since $\mathcal{L}$ is chosen such that $\mathcal{A}$ is Hurwitz, its exponential tends toward 0 when t tends toward infinity then: $\lim_{t\to+\infty} E(t) = \lim_{t\to+\infty} e^{\mathcal{A}t}E(0) = 0$. Statement $\mathbb{S}1$ is verified.

A.2. Proof of statement $\mathbb{S}2$

Since $\mathscr{C}^{(m)} \neq 0$, $\mathscr{C}^{(i)} \neq 0$ and therefore the dynamics of the estimation error (32) remains the same. It was shown in (Yang and Huang, 2009) that its solution is:

$$E\,(t) = e^{\mathcal{A}t}E(0) + \int_0^t e^{\mathcal{A}(t-\tau)}B_e\mathscr{C}^{(m)}(\tau)\mathrm{d}\tau \tag{A2}$$

which can be split into two parts:

$$R_1(t) = e^{\mathcal{A}t}E(0) \tag{A3}$$

and

$$R_2(t) = \int_0^t e^{\mathcal{A}(t-\tau)}B_e\mathscr{C}^{(m)}(\tau)\mathrm{d}\tau \tag{A4}$$

Since $\mathcal{A}$ is Hurwitz, $\lim_{t\to+\infty} R_1(t) = 0$. Consequently, in order to bound $\lim_{t\to+\infty} E(t)$, $\lim_{t\to+\infty} R_2(t)$ in (A4) has to be bounded.

Let us define the vector operator $|\,.\,|$ by:

$$\forall Q = \begin{bmatrix} q_1 \\ \vdots \\ q_\eta \end{bmatrix}, \qquad |\,Q\,| \triangleq \begin{bmatrix} |\,q_1\,| \\ \vdots \\ |\,q_\eta\,| \end{bmatrix} \tag{A5}$$

According to assumption 5.2, and knowing that $i = m$, we have $|\mathscr{C}^{(m)}| < \beta$, and then, using the operator $|\,.\,|$, it comes:

$$\lim_{t\to+\infty} |R_2(t)| \leq \beta \lim_{t\to+\infty} \left| \int_0^t e^{\mathcal{A}(t-\tau)} B_e \,\mathrm{d}\tau \right| \tag{A6}$$

The integral term in (A6) can be written as:

$$\begin{aligned} \int_0^t e^{\mathcal{A}(t-\tau)} B_e \,\mathrm{d}\tau &= \int_0^t -\mathcal{A}^{-1}(-\mathcal{A}e^{\mathcal{A}(t-\tau)}) B_e \mathrm{d}\tau \\ &= \mathcal{A}^{-1}e^{\mathcal{A}t}B_e - \mathcal{A}^{-1}B_e \end{aligned}$$

leading to:

$$\lim_{t\to+\infty} \left| \int_0^t e^{\mathcal{A}(t-\tau)} B_e \,\mathrm{d}\tau \right| = \lim_{t\to+\infty} \left| \mathcal{A}^{-1}e^{\mathcal{A}t}B_e - \mathcal{A}^{-1}B_e \right|$$

Therefore, $\lim\limits_{t\to+\infty} R_2(t)$ can be bounded by:

$$\lim_{t\to+\infty} |R_2(t)| \leq \beta \left| \mathcal{A}^{-1}B_e \right| + \beta \left(\lim_{t\to+\infty} \left| \mathcal{A}^{-1}e^{\mathcal{A}t}B_e \right| \right)$$

Again, since $\mathcal{A}$ is Hurwitz, we have

$$\lim_{t\to+\infty} \left| \mathcal{A}^{-1}e^{\mathcal{A}t}B_e \right| = 0 \tag{A7}$$

and the only term remaining to be bounded is $\left|\mathcal{A}^{-1}B_e\right|$.

According to the expressions of matrices A_e, C_e, $\mathcal{L}$ in (30) and the value of the gains in (35), the matrix $\mathcal{A}$ reads as:

$$\mathcal{A} = \begin{bmatrix} -\gamma_1\omega_o & 1 & \cdots & 0 & 0 & 0 & \cdots & 0 & 0 & \cdots & 0 & 0 \\ -\gamma_2\omega_o^2 & 0 & \ddots & 0 & 0 & 0 & \cdots & 0 & 0 & \cdots & 0 & 0 \\ \vdots & \vdots & & \ddots & & \vdots & & \vdots & \vdots & & \vdots & \vdots \\ -\gamma_{p-1}\omega_o^{p-1} & 0 & \cdots & 0 & 1 & 0 & \cdots & 0 & 0 & \cdots & 0 & 0 \\ -\gamma_p\omega_o^p & 0 & \cdots & 0 & a_p & 1 & & 0 & 0 & \cdots & 0 & 0 \\ -\gamma_{p+1}\omega_o^{p+1} & 0 & \cdots & 0 & a_{p-1} & 0 & \ddots & 0 & 0 & \cdots & 0 & 0 \\ \vdots & \vdots & & \vdots & \vdots & & & \ddots & & & \vdots & \vdots \\ -\gamma_{2p-1}\omega_o^{2p-1} & 0 & \cdots & 0 & a_1 & 0 & \cdots & 0 & 1 & & 0 & 0 \\ -\gamma_{2p}\omega_o^{2p} & 0 & \cdots & 0 & 0 & 0 & \cdots & 0 & 0 & \ddots & 0 & 0 \\ \vdots & \vdots & & \vdots & \vdots & \vdots & & \vdots & \vdots & & \ddots & \\ -\gamma_{p+m-1}\omega_o^{p+m-1} & 0 & \cdots & 0 & 0 & 0 & \cdots & 0 & 0 & \cdots & 0 & 1 \\ -\gamma_{p+m}\omega_o^{p+m} & 0 & \cdots & 0 & 0 & 0 & \cdots & 0 & 0 & \cdots & 0 & 0 \end{bmatrix} \tag{A8}$$

whose inverse $\mathcal{A}^{-1}$ is given by:

$$\mathcal{A}^{-1} = \begin{bmatrix}
0 & 0 & \cdots & 0 & 0 & 0 & \cdots & 0 & 0 & \cdots & 0 & -\frac{1}{\omega_o^{p+m}} \\
1 & 0 & \cdots & 0 & 0 & 0 & \cdots & 0 & 0 & \cdots & 0 & -\frac{\gamma_1}{\omega_o^{p+m-1}} \\
 & \ddots & & \vdots & \vdots & \vdots & & \vdots & \vdots & & \vdots & \vdots \\
0 & 0 & \ddots & 0 & 0 & 0 & \cdots & 0 & 0 & \cdots & 0 & -\frac{\gamma_{p-2}}{\omega_o^{p+m-(p-2)}} \\
0 & 0 & & 1 & 0 & 0 & \cdots & 0 & 0 & \cdots & 0 & -\frac{\gamma_{p-1}}{\omega_o^{p+m-(p-1)}} \\
0 & 0 & & -a_p & 1 & 0 & \cdots & 0 & 0 & \cdots & 0 & -\frac{a_p\gamma_{p-1} - \gamma_p\omega_o}{\omega_o^{p+m-(p-1)}} \\
\vdots & \vdots & & \vdots & & \ddots & & \vdots & \vdots & & \vdots & \vdots \\
0 & 0 & & -a_1 & 0 & 0 & \ddots & 0 & 0 & \cdots & 0 & -\frac{a_1\gamma_{p-1} - \gamma_{2p-1}\omega_o^p}{\omega_o^{p+m-(p-1)}} \\
0 & 0 & & 0 & 0 & 0 & & 1 & 0 & \cdots & 0 & -\frac{\gamma_{2p}}{\omega_o^{p+m-(2p)}} \\
\vdots & \vdots & & \vdots & \vdots & \vdots & & & \ddots & & \vdots & \vdots \\
0 & 0 & & 0 & 0 & 0 & & 0 & 0 & \ddots & 0 & -\frac{\gamma_{p+m-2}}{\omega_o^2} \\
0 & 0 & & 0 & 0 & 0 & & 0 & 0 & & 1 & -\frac{\gamma_{p+m-1}}{\omega_o}
\end{bmatrix} \tag{A9}$$

One can note that, in order to alleviate the notation in (A9), the term γ_{p+m} has been directly replaced by its value, i.e. 1, for $i = m$ and $j = p + m$.

Using the operator $|\,.\,|$ on the product of (A9) and B_e in (33) leads to: $\left|\mathcal{A}^{-1}B_e\right| \leq V + W$, where

$$\overbrace{\begin{bmatrix} \frac{|b|}{\omega_o^{p+m}} \\ \frac{|b|\,\gamma_1}{\omega_o^{p+m-1}} \\ \vdots \\ \frac{|b|\,\gamma_{p-2}}{\omega_o^{p+m-(p-2)}} \\ \frac{|b|\,\gamma_{p-1}}{\omega_o^{p+m-(p-1)}} \\ \frac{|b|\,|a_p\gamma_{p-1}-\gamma_p\omega_o|}{\omega_o^{p+m-(p-1)}} \\ \vdots \\ \frac{|b|\,|a_1\gamma_{p-1}-\gamma_{2p-1}\omega_o^p|}{\omega_o^{p+m-(p-1)}} \\ \frac{|b|\,\gamma_{2p}}{\omega_o^{p+m-(2p)}} \\ \vdots \\ \frac{|b|\,\gamma_{p+m-2}}{\omega_o^2} \\ \frac{|b|\,\gamma_{p+m-1}}{\omega_o} \end{bmatrix}}^{|\mathcal{A}^{-1}B_e|} \leq \overbrace{\begin{bmatrix} \frac{|b|}{\omega_o^{p+m}} \\ \frac{|b|\,\gamma_1}{\omega_o^{p+m-1}} \\ \vdots \\ \frac{|b|\,\gamma_{p-2}}{\omega_o^{p+m-(p-2)}} \\ \frac{|b|\,\gamma_{p-1}}{\omega_o^{p+m-(p-1)}} \\ \frac{|b|\,\gamma_p\omega_o}{\omega_o^{p+m-(p-1)}} \\ \vdots \\ \frac{|b|\,\gamma_{2p-1}\omega_o^p}{\omega_o^{p+m-(p-1)}} \\ \frac{|b|\,\gamma_{2p}}{\omega_o^{p+m-(2p)}} \\ \vdots \\ \frac{|b|\,\gamma_{p+m-2}}{\omega_o^2} \\ \frac{|b|\,\gamma_{p+m-1}}{\omega_o} \end{bmatrix}}^{V} + \overbrace{\begin{bmatrix} 0 \\ 0 \\ \vdots \\ 0 \\ 0 \\ \frac{|ba_p|\,\gamma_{p-1}}{\omega_o^{p+m-(p-1)}} \\ \vdots \\ \frac{|ba_1|\,\gamma_{p-1}}{\omega_o^{p+m-(p-1)}} \\ 0 \\ \vdots \\ 0 \\ 0 \end{bmatrix}}^{W} \tag{A10}$$

From (A10), it can be seen that:

$$V_j = \frac{|b|\,\gamma_{j-1}}{\omega_o^{p+m-(j-1)}} > 0 \tag{A11}$$

and

$$W_j \leq \epsilon = \frac{|b\overline{a}|\,\gamma_{p-1}}{\omega_o^{p+m-(p-1)}} > 0 \tag{A12}$$

where $\overline{a} = \max\{a_k\}_{k=1,\cdots,p}$, and $j = 1, \cdots, p+m$.

As a result, each term of $\left|\mathcal{A}^{-1}B_e\right|$ is bounded by:

$$\left|\left(\mathcal{A}^{-1}B_e\right)\right|_j = \left|\left(\mathcal{A}^{-1}B_e\right)_j\right| \leq V_j + \epsilon \tag{A13}$$

According to (A7) and (A13), the bound on $R_2(t)$ is:

$$\lim_{t\to+\infty}\left|R_{2_j}(t)\right| \leq \beta\,(V_j + \epsilon) \tag{A14}$$

and therefore

$$\lim_{t\to+\infty} |E_j(t)| \leq \beta\,(V_j + \epsilon) \tag{A15}$$

that can be written

$$\lim_{t\to+\infty} |E_j(t)| \leq \alpha_j, \qquad j = 1, \ldots, p+m, \tag{A16}$$

with $\alpha_j = \beta(V_j + \epsilon)$. Statement $\mathbb{S}2$ is verified.

A.3. Proof of statement $\mathbb{S}3$

In this case, $i < m$ and $\mathscr{C}^{(i)} = 0$. As in statement $\mathbb{S}1$, the dynamics of the estimation error in (32) can be written as:

$$\dot{E} = (A_e - \mathcal{L}C_e)E = \mathcal{A}E \tag{A17}$$

Therefore, with the same reasoning as in case of statement $\mathbb{S}1$, it can be easily shown that

$$\lim_{t\to+\infty} E(t) = \lim_{t\to+\infty} e^{\mathcal{A}t}E(0) = 0. \tag{A18}$$

Statement $\mathbb{S}3$ is verified.

A.4. Proof of statement $\mathbb{S}4$

The same demonstration as the one done for statement $\mathbb{S}2$ can be used to prove statement $\mathbb{S}4$. The only difference is that, as $i < m$, the dimensions of the matrices and vectors will be reduced from $p+m$ to $p+i$. Thus, it can be shown that

$$\lim_{t\to+\infty} |E_j(t)| \leq \zeta_j \tag{A19}$$

where $\zeta_j = \beta(V_j' + \epsilon')$. Statement $\mathbb{S}4$ is verified.

Appendix B. Proof of Theorem 5.5

The result in the case of statements $\mathbb{S}1$ and $\mathbb{S}3$ is obvious. In the case of statements $\mathbb{S}2$ and $\mathbb{S}4$, we note by $\gamma_j|_k$ and $\gamma_j|_i$ the coefficients associated to GeLESO$|_k$ and GeLESO$|_i$ respectively. According to (A10), the estimation error $\lim_{t\to+\infty} |E_j(t)|$ with $j = 1, \ldots, p+i$ is given by four different relations depending on the value of j. Indeed, the expression of the $\lim_{t\to+\infty} |E_j(t)|$ is different for:

- Case 1: index $j = 1$.
- Case 2: indices $j = 2, \ldots, p$.
- Case 3: indices $j = p+1, \ldots, p+i$ if $1 \leq i \leq p$.
- Case 4: indices $j = 2p+1, \ldots, p+i$ if $i > p$.

Let us now compare $\lim_{t\to+\infty}|E_j(t)|$ generated by GeLESO$|_k$ and GeLESO$|_i$ for each case.

B.1. Case 1: index $j = 1$

In that case, according to (A10), $\lim_{t\to+\infty}|E_1(t)|_i = \frac{|b|}{\omega_o^{p+i}}$ and $\lim_{t\to+\infty}|E_1(t)|_k = \frac{|b|}{\omega_o^{p+k}}$.
To compare $\lim_{t\to+\infty}|E_1(t)|_i$ and $\lim_{t\to+\infty}|E_1(t)|_k$, it suffices to calculate:

$$\frac{\lim_{t\to+\infty}|E_1(t)|_k}{\lim_{t\to+\infty}|E_1(t)|_i} = \frac{\frac{|b|}{\omega_o^{p+k}}}{\frac{|b|}{\omega_o^{p+i}}} = \frac{1}{\omega_o^r}, \quad \text{with } r = k - i > 0. \tag{B1}$$

Therefore, for all $\omega_o > 1$, we have $\frac{\lim_{t\to+\infty}|E_1(t)|_k}{\lim_{t\to+\infty}|E_1(t)|_i} < 1$.
This verifies that $\lim_{t\to+\infty}|E_1(t)|_k < \lim_{t\to+\infty}|E_1(t)|_i$, for $\omega_o > 1$.

B.2. Case 2: indices $j = 2, \ldots, p$

In that case, still according to (A10), $\lim_{t\to+\infty}|E_j(t)|_i = |b|\frac{\gamma_{j-1}|_i}{\omega_o^{p+i-(j-1)}}$ and $\lim_{t\to+\infty}|E_j(t)|_k = |b|\frac{\gamma_{j-1}|_k}{\omega_o^{p+k-(j-1)}}$.
To compare $\lim_{t\to+\infty}|E_j(t)|_i$ and $\lim_{t\to+\infty}|E_j(t)|_k$, it suffices to calculate:

$$\frac{\lim_{t\to+\infty}|E_j(t)|_k}{\lim_{t\to+\infty}|E_j(t)|_i} = \frac{|b|\frac{\gamma_{j-1}|_k}{\omega_o^{p+k-(j-1)}}}{|b|\frac{\gamma_{j-1}|_i}{\omega_o^{p+i-(j-1)}}}.$$

Let $r = k - i > 0$. The coefficients γ_j are calculated using (36).

$$\frac{\lim_{t\to+\infty}|E_j(t)|_k}{\lim_{t\to+\infty}|E_j(t)|_i} = \frac{\Xi_2}{\omega_o^r} \tag{B2}$$

with $\Xi_2 = \frac{(p+k)!(p+i-j)!}{(p+k-j)!(p+i)!}$.

Therefore, for all $\omega_o > \sqrt[r]{\Xi_2}$, we have $\frac{\lim_{t\to+\infty}|E_j(t)|_k}{\lim_{t\to+\infty}|E_j(t)|_i} < 1$.

This verifies that $\lim_{t\to+\infty}|E_j(t)|_k < \lim_{t\to+\infty}|E_j(t)|_i$, for $j = 2, \ldots, p$ and $\omega_o > \sqrt[r]{\Xi_2}$.

B.3. Case 3: indices $j = p+1, \ldots, p+i$ with $1 \leq i \leq p$

In that case, still according to (A10):

$$\lim_{t\to+\infty} |E_j(t)|_k = |b|\frac{\gamma_{j-1}|_k}{\omega_o^{p+k-(j-1)}} + |ba_{2p-(j-1)}|\frac{\gamma_{p-1}|_k}{\omega_o^{p+k-(p-1)}} \tag{B3}$$

and

$$\lim_{t\to+\infty} |E_j(t)|_i = |b|\frac{\gamma_{j-1}|_i}{\omega_o^{p+i-(j-1)}} + |ba_{2p-(j-1)}|\frac{\gamma_{p-1}|_i}{\omega_o^{p+i-(p-1)}}. \tag{B4}$$

The same procedure as the one used in the case 2 for the comparison between $\lim_{t\to+\infty} |E_j(t)|_k$ and $\lim_{t\to+\infty} |E_j(t)|_i$ will be used again to compare the left parts of (B3) and (B4), i.e., $|b|\frac{\gamma_{j-1}|_k}{\omega_o^{p+k-(j-1)}}$ and $|b|\frac{\gamma_{j-1}|_i}{\omega_o^{p+i-(j-1)}}$. So, for all $\omega_o > \sqrt[r]{\Xi_2}$, we have

$$|b|\frac{\gamma_{j-1}|_k}{\omega_o^{p+k-(j-1)}} < |b|\frac{\gamma_{j-1}|_i}{\omega_o^{p+i-(j-1)}} \tag{B5}$$

Now, let us compare the ratio between the right part of (B3) and (B4):

$$\frac{|ba_{2p-(j-1)}|\frac{\gamma_{p-1}|_k}{\omega_o^{p+k-(p-1)}}}{|ba_{2p-(j-1)}|\frac{\gamma_{p-1}|_i}{\omega_o^{p+i-(p-1)}}} = \frac{\Xi_3}{\omega_o^r} \tag{B6}$$

with $\Xi_3 = \dfrac{(p+k)!(i+1)!}{(k+1)!(p+i)!}$.

Then, for all $\omega_o > \sqrt[r]{\Xi_3}$, we have

$$|ba_{2p-(j-1)}|\frac{\gamma_{p-1}|_k}{\omega_o^{p+k-(p-1)}} < |ba_{2p-(j-1)}|\frac{\gamma_{p-1}|_i}{\omega_o^{p+i-(p-1)}}.$$

Consequently, $\lim_{t\to+\infty} |E_j(t)|_k < \lim_{t\to+\infty} |E_j(t)|_i$, for all $\omega_o > \max\left\{\sqrt[r]{\Xi_2}, \sqrt[r]{\Xi_3}\right\}$.

B.4. Case 4: indices $j = 2p+1, \ldots, p+i$ if $i > p$

In that case, still according to (A10), $\lim_{t\to+\infty} |E_j(t)|_i = |b|\frac{\gamma_{j-1}|_i}{\omega_o^{p+i-(j-1)}}$ and $\lim_{t\to+\infty} |E_j(t)|_k = |b|\frac{\gamma_{j-1}|_k}{\omega_o^{p+k-(j-1)}}$ which are the same as in case 2. Therefore, with the same reasoning as in case 2, it can be easily shown that $\lim_{t\to+\infty} |E_j(t)|_k < \lim_{t\to+\infty} |E_j(t)|_i$, for $j = 2p+1, \ldots, p+i$ and $\omega_o > \sqrt[r]{\Xi_2}$.

Let us define

$$\omega_{max} \triangleq \max\left\{1, \sqrt[r]{\Xi_2}, \sqrt[r]{\Xi_3}\right\}. \tag{B7}$$

Regarding the four studied cases, (38) has been proven for all $j = 1, \ldots, p+i$ if $\omega_o > \omega_{max}$.

From (21), the estimation of the virtual input $\hat{\mathscr{C}}$ is a linear combination of the estimation of the components of X_e. As these components are better estimated when the order of the GeLESO increases, it is the same for the estimation of the virtual input.